Mendeleev Commun., 2027, **37**, JUST ACCEPTED

Received 03.09.26
Revised 06.10.26

26/8191

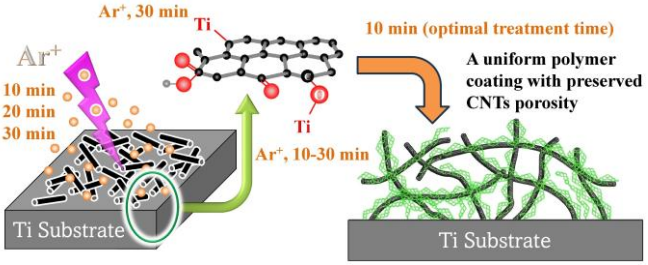
Control of the morphology of a poly[Ni(salen)] coating on multi-walled carbon nanotubes/Ti by varying ion irradiation of the substrate

Petr M. Korusenko,*[a,b,c] Egor V. Knyazev, [c,d] Denis V. Sokolov, [c,d] Anatoliy A. Vereshchagin,[e] Oleg V. Levin[a] and Alexander S. Vinogradov[a]

[a] *St. Petersburg State University, 199034 St. Petersburg, Russian Federation. E-mail: p.korusenko@spbu.ru*
[b] *National Research Nuclear University MEPhI, 115409 Moscow, Russian Federation*
[c] *Omsk State Technical University, 644050 Omsk, Russian Federation*
[d] *Omsk Scientific Centre, Siberian Branch of the Russian Academy of Sciences, 644013 Omsk, Russian Federation*
[e] *Freie Universität Berlin, 14195 Berlin, Germany*

DOI: 10.71267/mencom.8191

A systematic study of argon ion irradiation (10–30 min) of multi-walled carbon nanotube (MWCNT) layers on titanium reveals that 10 min treatment optimally enhances interfacial adhesion by forming C–O–Ti bonds while preserving the nanotube network integrity. This modified surface changes the growth mode of poly-[Ni(Salen)] polymer from island to layer-plus-island, yielding a thinner, more uniform coating without blocking the porous structure. The results demonstrate a solvent-free route for tailoring the morphology of metal-salen polymer/carbon nanotube composites, which is important for the development of high-performance binder-free supercapacitor electrodes.



Keywords: multi-walled carbon nanotubes (MWCNTs), poly-[Ni(Salen)] polymer, ion-beam treatment, composite, morphology, adhesion measurement.

Recent studies have highlighted the potential of nanostructured and composite materials for supercapacitor electrodes, owing to their ability to combine complementary charge-storage and transport properties.[1-3] In this context, composites combining conducting Ni-Salen-type polymers with multi-walled carbon nanotubes (MWCNTs) are promising candidates for supercapacitor electrodes, where the Ni-Salen polymer provides pseudocapacitive charge storage through reversible redox processes, while the MWCNT network promotes electron transport and provides a large accessible surface for electrochemical reactions.[4-11] However, the poor adhesion of the polymer to the inert nanotube surface leads to uncontrolled morphology of the polymer layer and a deterioration of its properties.[11,12] Ion-beam treatment of the MWCNTs/Ti substrate offers an environmentally friendly alternative to acid functionalization and improves adhesion by creating chemically active surface defects and oxygen-containing functional groups.[13] Nevertheless, the effect of irradiation time on the morphology of the MWCNTs layer, interfacial adhesion strength and chemical composition of the interface, as well as on the subsequent electrochemical deposition of poly-[Ni(Salen)], remain unexplored.

In the present work, we systematically investigate argon ion irradiation (10, 20 and 30 min) of MWCNTs/Ti substrates using scanning electron microscopy (SEM), atomic force microscopy (AFM) and X-ray photoelectron spectroscopy (XPS). The main aim of this study is to determine the optimal irradiation regime that ensures maximum interfacial adhesion while preserving nanotube layer integrity, which will make it possible to form poly-[Ni(Salen)]/MWCNTs/Ti composites with tailored morphology.

Detailed information on the preparation of the MWCNTs/Ti substrates, Ar^+ irradiation, fabrication of the poly-[Ni(Salen)]/MWCNTs composites, as well as the experimental procedures and instrumentation used for their characterization, is provided in the footnote below and in our previous works.[13,14] †

SEM images (Figure 1a–d) reveal that increasing irradiation time from 10 to 30 min progressively damages the nanotube layer. After 10 min, only minor morphological

† A layer of commercial MWCNTs (outer diameter 4–21 nm, specific surface 250 $m^2 \cdot g^{-1}$) was deposited onto Ti foil (thickness ~1 μm) using the aerosol spraying method. Irradiation with Ar^+ (20 keV, 10, 20 and 30 min) was carried out using an ion implanter. Poly-[Ni(Salen)]/MWCNTs composites were prepared on MWCNTs/Ti substrates before and after ion irradiation. The electrolyte solution contained 0.001 M [Ni(Salen)] and 0.1 M $LiBF_4$ in acetonitrile. Electropolymerization was performed using an Elins P 45X potentiostat/galvanostat in a three-electrode cell with the MWCNTs/Ti substrate as the working electrode (area ~7 cm^2). Initially, two cyclic voltammetry (CV) cycles were run in the potential range from –0.2 to +1.0 V at a scan rate of 50 mV s^{-1} to activate the surface. Subsequently, a constant potential of +1.0 V was applied until the desired charge density ($C \cdot cm^{-2}$) was reached; for example, a charge density of 0.0075 $C \cdot cm^{-2}$ corresponds to a polymer film thickness of ~450–500 nm on a planar Ti substrate.Morphology was examined by SEM (Jeol JSM 6610-LV and Carl Zeiss Merlin electron microscope), adhesion force was measured by contact AFM (MFP-3D, HA_HR cantilevers, k ~34 N/m), and XPS spectra were recorded using an ESCALAB 250 Xi spectrometer (Thermo Fisher Scientific, UK) with a monochromatic Al Kα source. Detailed measurement conditions for all techniques are described in our previous works.[13,14]

© Mendeleev Communications.

changes are observed. Extension to 20 min induces the formation of voids (500–800 nm) and partial fusion of adjacent nanotubes. The most severe alterations occur at 30 min, indicating considerable deterioration of layer integrity during prolonged ion exposure.

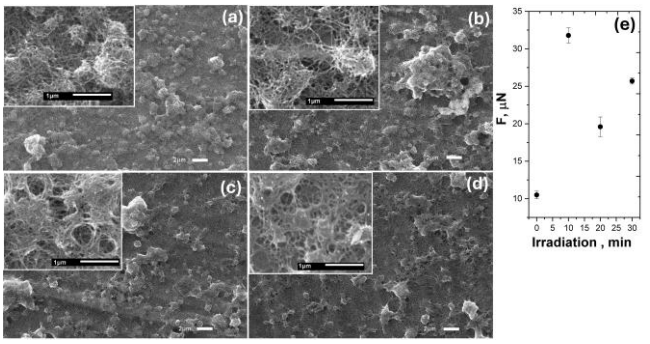


Figure 1 SEM images of the MWCNTs/Ti layer: (a) initial sample, after Ar^+ irradiation for 10 min (b), 20 min (c), 30 min (d). Average interfacial adhesion force values as a function of irradiation time (e), error bars represent standard deviations.

Measurements of adhesion force were performed by AFM in the contact mode. The surface of the MWCNTs layer was scanned at a rate of 50 μm/s with loading forces ranging from 0.3 to 40 μN, increasing stepwise by 0.2 μN per scan. Layer failure was detected visually by the appearance of reflected light from the Ti substrate within scan area using an optical camera (×400 magnification). The adhesion force *F* (μN) was determined from the deflection signal (*DFL*, V) of the laser-optical cantilever system as $F = k \cdot \Delta z \cdot DFL$, where *k* is the cantilever spring constant and Δ*z* is the slope of the experimental force-distance curve (nm/V). AFM measurements (Figure 1e) show a significant increase the adhesion force after only 10 min of irradiation, from 10±0.5 μN for the initial sample to 31.8±1.0 μN. Longer treatment results in lower values (19.6±1.3 μN and 25.7±0.4 μN for 20 and 30 min, respectively). Thus, the 10 min regime combines maximum adhesion enhancement with minimal structural damage.

The analysis of XPS spectra (Figure 2) elucidates the origin of the improved adhesion. In the C 1*s* spectra of irradiated samples, line broadening (FWHM increases from 0.7 eV for the initial sample to 1.7 eV after 30 min of Ar^+ irradiation), redistribution of component intensities and disappearance of the *shake-up* satellite are observed – all of which are indicative of defect formation and generation of oxygen-containing groups (C–O, C=O, COOH) on the nanotube walls. For the 30 min regime, an additional component appears at ~282.2 eV, assigned to direct C–Ti bonding,[15,16] which is absent for shorter irradiation times. The O 1*s* spectra of the irradiated samples show pronounced broadening and a modified lineshape compared to the initial sample. This is attributed to an increase in the relative intensities of the components corresponding to oxygen in single (O–C at ~533.1 eV)[13] and double (O=C at ~532.1 eV)[13] carbon–oxygen bonds. For the 10 and 20 min Ar^+ treatments, the O–C and O=C components are enhanced, with the highest intensity of the O–C component recorded for the 10 min regime, which directly correlates with the adhesion maximum (Figure 1e). After 30 min of Ar^+ irradiation, a noticeable decrease in the relative intensities of both components is observed, which may result from ion-stimulated formation and subsequent destruction of O–C/O=C groups at irradiation-induced defect sites. It is noteworthy that the Ti 2*p* spectra (not shown) exhibit no C–Ti component (455–456 eV)[15,16] for 10 and 20 min treatments, whereas weak signs of direct C–Ti bonding appear after 30 min, accompanied by a corresponding C 1*s* component at ~282.2 eV (Figure 2). Seemingly, it is the formation of these direct C–Ti bonds that leads to a certain increase in interfacial adhesion for the 30 min irradiated sample compared to the 20 min one. This indicates that for the optimal 10 min regime, adhesion enhancement is primarily governed by the formation of interfacial C–O–Ti bonds between titanium substrate atoms and oxygen-containing groups at defect sites on the surface of the nanotubes, rather than by Ti–C formation.

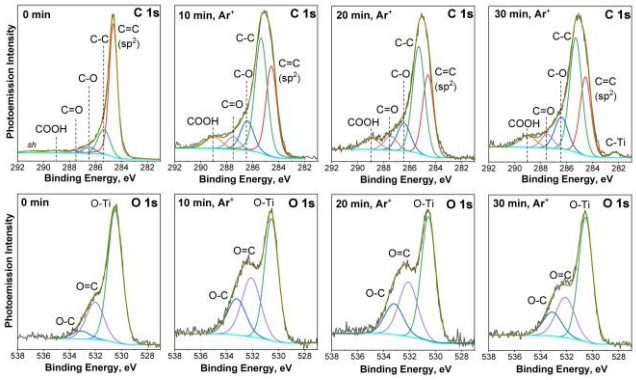


Figure 2 C 1*s* and O 1*s* photoelectron spectra of the MWCNTs/Ti system before and after Ar^+ irradiation for 10, 20 and 30 min.

Based on the combined evidence, the 10 min irradiation regime provides the most favorable balance between interfacial adhesion enhancement and preservation of the MWCNT layer structure. At this irradiation time, the adhesion force reaches its maximum, while the MWCNT layer retains comparatively low morphological damage and the surface exhibits the highest concentration of oxygen-containing C–O functional groups, which are associated with the formation of interfacial C–O–Ti bonds. Further irradiation increases structural damage and reduces the concentration of oxygen-containing groups without improving adhesion. Therefore, 10 min provides the best balance between interfacial adhesion enhancement and preservation of the MWCNT layer and was selected as the optimal regime for composite fabrication.

Subsequently, poly-[Ni(Salen)]/MWCNTs/Ti composites were prepared on both initial and irradiated (10 min) substrates. The repeating structural fragment of poly-[Ni(Salen)] is shown in Figure 3e, while a more detailed discussion of the polymer structure in the reduced and oxidized states was provided in our previous work.[17] SEM images (Figure 3) reveal a striking difference in polymer morphology on these substrates. On the initial MWCNTs/Ti substrate (Figure 3a, c), the nanotubes form a continuous porous network (average MWCNTs diameter ~10.7 nm). Polymer deposition proceeds via an island (Volmer–Weber) mechanism: large globules (50–120 nm) nucleate on individual nanotubes, gradually encapsulating them and filling intertubular voids. Consequently, the average diameter of polymer-coated nanotubes increases to ~139.4 nm, pores become largely blocked, and the estimated coating thickness reaches ~64 nm, indicating substantial porosity loss.

In contrast, on the Ar^+-irradiated substrate (irr-MWCNTs/Ti, Figure 3b, d), polymer growth follows a layer-plus-island (Stranski–Krastanov) mechanism. At the initial stage, the growth occurs layer-by-layer, which ensures a more uniform and continuous coating, as can be seen in the inset in Figure 3d (fragment after the first two CV cycles). Globule size decreases to 50–90 nm, the average coated nanotube diameter is ~107 nm, and the coating thickness is reduced to ~42

© Mendeleev Communications.

nm. Importantly, the porous network of the nanotube layer is largely preserved. This morphological transition is explained by the presence of ion-induced surface defects and oxygen-containing groups, which serve as preferential nucleation sites and improve surface wettability, thereby facilitating the formation of a homogeneous film.

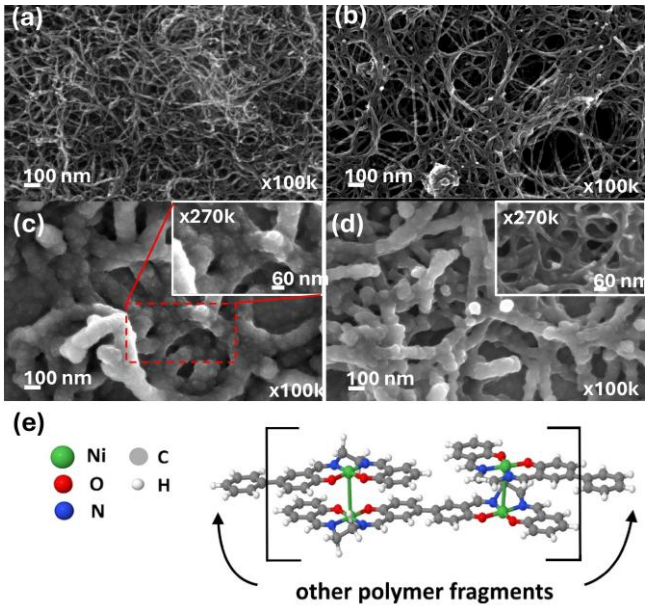


Figure 3 SEM images of the surface layer of samples: (a) initial MWCNTs/Ti system; (b) MWCNTs/Ti after Ar^+ irradiation for 10 min (irr-MWCNTs/Ti); (c) poly-[Ni(Salen)] composite on MWCNTs/Ti (inset shows an enlarged fragment); (d) poly-[Ni(Salen)] composite on irr-MWCNTs/Ti (inset shows a fragment after the first 2 CV polymerization cycles); (e) repeating structural fragment of poly-[Ni(Salen)].

Thus, a systematic investigation of morphology, adhesion properties and chemical state of the MWCNTs/Ti system after argon ion irradiation has established 10 min as the optimal treatment time. This regime provides a three-fold increase in interfacial adhesion while causing minimal damage to the nanotube layer. The adhesion enhancement arises primarily from the formation of interfacial C–O–Ti bonds, rather than from Ti–C formation, as confirmed by XPS. Importantly, the pre-irradiated substrate modifies the poly-[Ni(Salen)] growth mechanism from island to layer-plus-island, yielding a thinner, more uniform coating with preserved porosity, which should favor electrolyte-ion transport and accessibility of electrochemically active sites and may contribute to enhanced pseudocapacitive performance. In addition, the improved interfacial adhesion at the MWCNT–Ti interface may facilitate more efficient charge transfer from the polymer through the MWCNT network to the Ti substrate. These findings offer a solvent-free, scalable approach for fabricating metal-salen polymer/carbon nanotube composites with controlled morphology, which is important for advanced binder-free supercapacitor electrodes.

This research was funded by the Russian Science Foundation (grant no. 25-22-00583) for preparation of initial and irradiated systems, morphology analysis, and adhesion characterization by AFM and XPS. Other parts were supported by the Ministry of Science and Higher Education of the Russian Federation (project No. FSWU-2024-0014).

References

1 Simonenko N.P., Simonenko T.L., Arsenov P.V. and Simonenko E.P., *Mendeleev Commun.*, 2026, **36**, 481–483. https://doi.org/10.71267/mencom.7969.
2 Zhao L., Yu X., Xiong Z., Wang K., Cui R., Wang Z., Li Y. and Lei Y., *Electrochim. Acta*, 2026, **510**, 148502. https://doi.org/10.1016/j.electacta.2026.148502.
3 Mahimai B.M., Li E., Pang J., Zhang J. and Zhang J., *J. Energy Storage*, 2024, **96**, 112598. https://doi.org/10.1016/j.est.2024.112598.
4 Li X., Deng F., Li J., Li Z. and Kang F., *Electrochim. Acta*, 2018, **284**, 355–365; https://doi.org/10.1016/j.electacta.2018.07.065.
5 Alekseeva E.V., Stelmashuk T.A., Ershov V.A. and Levin O.V., *Electrochim. Acta*, 2021, **383**, 138309. https://doi.org/10.1016/j.electacta.2021.138309.
6 G. Yan, J. Li, Y. Zhang, F. Gao and F. Kang, *J. Phys. Chem. C*, 2014, **118**, 9911–9917; https://doi.org/10.1021/jp500249t.
7 C. Chen, Z. Zhu, X. Li and J. Li, *J. Appl. Polym. Sci.*, 2016, **134**, 44480; https://doi.org/10.1002/app.44480.
8 Y. Zhang, J. Li, F. Gao, F. Kang, X. Wang, F. Ye and J. Yang, *Electrochim. Acta*, 2012, **76**, 1–7; https://doi.org/10.1016/j.electacta.2012.03.182.
9 Z. Zhu, J. Lu, X. Li, G. Xu, C. Chen and J. Li, *Electrochemistry*, 2016, **84**, 427–431; https://doi.org/10.5796/electrochemistry.84.427.
10 J. Li, F. Gao, Y. Zhang, F. Kang, X. Wang, F. Ye and J. Yang, *Sci. China Chem.*, 2012, **55**, 1338–1344; https://doi.org/10.1007/s11426-012-4585-y.
11 J. Tedim, F. Gonçalves, M. J. Pereira, J. F. Figueiredo, C. Moura, C. Freire and A. R. Hillman, *Electrochim. Acta*, 2008, **53**, 6722–6731; https://doi.org/10.1016/j.electacta.2008.01.079.
12 P. M. Korusenko, O. V. Petrova and A. S. Vinogradov, *Appl. Sci.*, 2024, **14**, 1178; https://doi.org/10.3390/app14031178.
13 P.M. Korusenko, E.V. Knyazev, O.V. Petrova, D.V. Sokolov, S.N. Povoroznyuk, K.E. Ivlev, K.A. Bakina, V.A. Gaas and A.S. Vinogradov, *Nanomaterials*, 2024, **14**, 699; https://doi.org/10.3390/nano14080699.
14 P. Korusenko, K. Kharisova, E. Knyazev, O. Levin, A. Vinogradov and E. Alekseeva, *Appl. Sci.*, 2023, **13**, 11057; https://doi.org/10.3390/app131911057.
15 H. Belhadj, I. Moulefera, L. Sabantina, A. Benyoucef. *Fibers*, 2022, **10**, 46; https://doi.org/10.3390/fib10050046.
16 Z. Xiang, Y. Shi, X. Zhu, L. Cai and W. Lu, *Nano-Micro Lett.*, 2021, **13**, 150; https://doi.org/10.1007/s40820-021-00673-9.
17 P.M. Korusenko, O.V. Petrova, A.A. Vereshchagin, O.V. Levin, E.V. Khramov, R.G. Chumakov, M.A. Soldatov, K.P. Katin, A.S. Konev and A.S. Vinogradov, *Phys. Chem. Chem. Phys.*, 2025, **27**, 15080–15098. https://doi.org/10.1039/D5CP01410G

Received: 3rd September 2026; Com. 26/8191

© Mendeleev Communications.